Some features of phase transition in chromium arsenide at high pressures

É. A. Zavadskiĭ and I. A. Sibarova

Donetsk Physicotechnical Institute, Ukrainian Academy of Sciences
(Submitted 10 July 1979)
Zh. Eksp. Teor. Fiz. **78**, 1076–1086 (March 1980)

The effect of hydrostatic pressure up to 9 kbar on the electric properties of chromium arsenide is investigated in a wide temperature interval, 4.2–350 K. It is found that up to 3.2 kbar the temperature of the antiferromagnetism-paramagnetism phase transition shifts toward higher temperatures at a rate $dT_N/dp = -18$ deg/kbar. With further increase of pressure the anomalies on the $R(T)/R_0$ curves decrease and vanish completely at $P > 4.5$ kbar. A band model of chromium arsenide is constructed on the basis of the experimental data and of the conclusions of the crystal-field theory. The model explains the metallic character of the conduction, the helicoidal magnetic ordering in the low-temperature phase, and the effect of pressure on the shift of T_N in CrAs. In light of this model, a mechanism is proposed for the first-order phase transition in this compound. A two-band formula is used to calculate the width of the d-band which determines the principal magnetic and electric properties of chromium arsenide, and its variation under pressure.

PACS numbers: 64.70.Kb, 72.15.Eb, 61.50.Em

1. INTRODUCTION

Monoarsenides of transition metals have long attracted the attention of researchers because of a number of interesting crystallographic and magnetic properties. All have either a nickel arsenide lattice ($B8_1$), or crystallize into a structure of the MnP type ($B31$), which differs from that indicated above in having orthorhombic distortions. The character and degree of distortion of these compounds are responsible for the singularities of the magnetic structures. The structural transitions $B8_1 \rightleftarrows B34$ and the magnetic transitions yield extensive information on the exchange interactions that determine these singularities.

Chromium arsenide stands out from among these substances in that it undergoes a first-order magnetic phase transition of the antiferromagnetism—paramagnetism (AF-PM) type in the 265 K region. This transition is not accompanied by a change in the symmetry of the crystal lattice. Both before and after the transition, CrAs has a $B31$ structure.[1] Neutron-diffraction investigations have shown[1] that at temperatures below 265 K a magnetic structure of the double-helix (DH) type is realized in CrAs.

The crystalline and magnetic structures of CrAs were investigated in detail in Ref. 2. It was observed that the helicoidal magnetic ordering in this substance differs from the double helices of other monoarsenides in that the angle between the spins of the atoms belonging to different helices is 183.5°, i.e., a strong antiferromagnetic coupling exists between these atoms and in fact determines the antiferromagnetic properties of CrAs. In the same paper, the authors investigated the behavior of the magnetic susceptibility and found that above the Neel temperature T_N it is practically independent of temperature. This is evidence that CrAs is in this region a Pauli paramagnet.

Boller and Kallel[3] carried out x-ray diffraction and neutron-diffraction investigations of the phase transition in CrAs. It turned out that even though the symmetry of the crystal lattice is not altered by the phase transition, the transition is accompanied by a large jumplike and anisotropic change in the volume of the unit cell ($\Delta V/V \approx 3.7\%$). Recognizing that CrAs has a magnetic moment $1.7\mu_B$ below T_N and is a Pauli paramagnet above T_N, they treat the first-order transition in CrAs as a transformation accompanying the transition of the $3d$ electrons from a localized to a collectivized state (LS → CS) transition. Since this transition is inseparable from a change in the interatomic distances, it is of particular interest to investigate the influence of hydrostatic pressure on the properties of CrAs.

In our first paper[4] we investigated the influence of hydrostatic pressure up to 2 kbar on the shift of T_N, as determined from measurements of the electric conductivity and the heat released in the phase transition. It was found that T_N shifts towards lower temperatures with increasing pressure at a rate $dT_N/dp = -19.5$ deg/kbar. This experimental value agrees well with the calculated $(dT_N/dP)_{calc} = -19$ deg/kbar obtained from calculations based on the Bean and Rodbell exchange-striction model.[5]

In our next study[6] we observed that under the influence of pressure the anomalies of the transition become smoothed out on the electric-conductivity curves, and at $P = 4.5$ kbar the transition vanishes completely. This was attributed to the fact that at this pressure the interatomic distances decrease to a critical value such that the interaction of the localized electrons in the low-temperature phase no longer satisfies the Friedel criterion, the $3d$ electrons become collectivized, and the phase transition vanishes.

Among the monoarsenides of transition metals, constant attention is being paid to MnAs, the singularities of the magnetic, crystallographic, and other properties of which are the subject of numerous theoretical and experimental papers. In particular, a model of the band structure of MnAs was proposed in Ref. 7 and explains the magnetic and electric properties of this compound on the basis of the crystal-field theory. We attempted

 0038-5646/80/030542-06$02.40

to ascertain the character of the first-order phase transition in CrAs, as well as its magnetic and electric properties, by using this model for the construction of the band scheme of CrAs.

Since the change of the electric properties of a substance is inseparably connected with a restructuring of the electron spectrum, and the analysis of the electric conductivity curves as functions of the temperature yields information on the state of the $3d$ electrons, we have undertaken in the present study a new investigation of the electric conductivity of CrAs in a large temperature interval 4.2 – 350 K, under the action of a high hydrostatic pressure up to 9 kbar.

2. PREPARATION OF SAMPLES AND EXPERIMENTAL PROCEDURE

The CrAs samples were made of chromium and arsenic of high purity. To prevent oxidation we weighted the components and mixed and ground them in a special vacuum box in the atmosphere purified argon. The mixture was placed in quartz ampoules, evacuated to 10^{-5} Torr, and sintered for 10 days at 1100 °C. The temperature was raised slowly (10 – 15 deg/hr), to prevent bursting of the ampoules as a result of the intense sublimation of the arsenic. After sintering, the samples were ground and annealed again under the same conditions, to increase their homogeneity.

The obtained samples were too brittle to measure the electric properties and crumbled in the first-order phase transition because of the large change in volume. They were therefore melted in an induction furnace in evacuated quartz ampoules at $T \sim 1200°$ C, and then annealed for 50 hours at $T \sim 900$ °C. The finished samples were checked by x-ray structure analysis.

The electric resistance was measured by a four-contact method. The hydrostatic compression was effected in a high-pressure container with inside diameter 8.5 mm. The container was placed in a helium cryostat, which could change the temperature of the sample in a wide range, 4.2 – 350 K. The sample was cooled or heated slowly (at a rate 2.5 deg/min) in view of its cracking in the transition.

3. EXPERIMENTAL RESULTS

Figure 1 shows plots of $R(T)/R_0$, where R_0 is the resistance at $T = 350$ K, plotted at various hydrostatic pressures. As seen from the figure, the pressure shifts the transition temperature T_N towards lower temperatures. Up to 3.2 kbar, the shift of T_N has a practically linear dependence on the pressure, and the temperature hysteresis ~10 K remains unchanged. At $P = 4$ kbar the anomalies on the curves become smoothed out, and at $P = 4.75$ kbar they are too small to determine from them the transition temperature. Nonetheless, with increasing pressure the temperature hysteresis increases to 25 K at $P = 4.75$ kbar. At higher pressures, up to 9 kbar, no anomalies have been observed on the $R(T)/R_0$ plots, which were linear in the entire investigated temperature interval.

Chromium arsenide has metallic conductivity in the

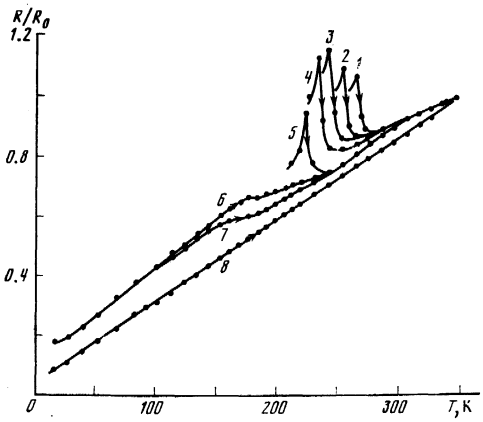

FIG. 1. Plots of $R(T)/R_0$ at various pressures P, kbar: 1—0; 2—0.75; 3—1.4; 4—2.2; 5—3.2; 6—4.3; 7—4.9; 8—9.0.

entire range of pressures and temperatures. In order not to clutter up Fig. 1, the low-temperature parts of the $R(T)/R_0$ plots at pressures up to 3.2 kbar are not shown. All are linear, starting with 30 K, but their slopes do not remain constant when the pressure is varied. At atmospheric pressure $d(R/R_0)/dT = 0.0044$ deg^{-1} and at $P = 3.2$ kbar $d(R/R_0)/dT = 0.0038$ deg^{-1}. With increasing pressure, the derivative decreases gradually and finally $d(R/R_0)/dT = 0.0028$ deg^{-1} at $P = 9$ kbar. In the high-temperature region the slopes of the curves, on the contrary, increase from 0.0020 deg^{-1} at atmospheric pressure to a value $d(R/R_0)/dT = 0.0028$ deg^{-1} at $P = 9$ kbar. This behavior of the linear sections of the $R(T)/R_0$ plots yields additional information on the state of the $3d$ electrons in CrAs, and their analysis will be presented below (sec. 4B).

The measured temperature dependences of the electric resistance were used to plot the $P - T$ phase diagram of CrAs (Fig. 2). It is seen from this figure that T_N up to $P = 3.5$ kbar depends linearly on the pressure, with $dT_N/dP = -18$ deg/kbar, after which the slope changes, and above 3.5 kbar we have $dT_N/dP = -47$ deg/kbar. Despite the small value and diffuse character of the anomalies on curves 6 and 7 of Fig. 1, they cannot offer evidence that the LS → CS transition becomes of

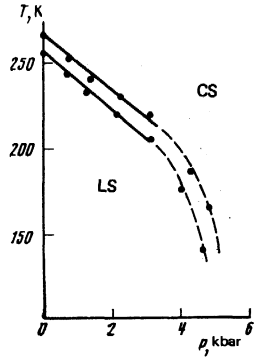

FIG. 2. $P-T$ phase diagram of chromium arsenide obtained from measurements of the electric resistance. The experimental points of the upper curve correspond to the transition temperature T_N when the sample is heated, and the points of the lower curve correspond to cooling; LS—region of localized state of the electrons, CS—region of collectivized state of the electrons.

second order, since the temperature hysteresis not only fails to vanish with increasing pressure, but even increases somewhat. Obviously we are dealing with a closed helicoidal magnetic phase bounded by a metastable region, and at $P = 4.5$ kbar this phase vanishes, again via a first-order phase transition. At this pressure we find ourselves at the boundary of the LS phase and, as will be shown below (sec. 4B), the anomalies on the curves 6 and 7 are connected with the redistribution of the collectivized electrons with the d bands of CrAs. Therefore the phase-diagram points obtained from these curves are connected by dashed curves.

4. DISCUSSION OF RESULTS

A. Band model of chromium arsenide

As indicated in Sec. 1, the aggregate of the electric and magnetic properties of CrAs allows us to assume that at 265 K a phase transition of the $3d$ electrons from the LS to the CS takes place. Boller and Kallel[3] were the first to suggest a qualitative band scheme for the low-temperature (LT) and the high-temperature (HT) phases of CrAs at atmospheric pressure. The scheme was based on the crystal-field theory was subsequently developed by Goodenough to explain the magnetic properties of transition-metal oxides and of manganese arsenide and phosphide.[7-10] We have attempted to construct the band scheme of CrAs in light of the same model concepts, but with account taken of direct (electric, magnetic, etc.) experimental data.

The band scheme must take into account the following: a) the matallic character of the electric conductivity of CrAs in the LT and HT phases; b) the presence in the LT phase of a localized magnetic moment $1.7\mu_B$ per chromium atom and the helicoidal magnetic ordering in this phase; c) the large anisotropic change of the interatomic distances in CrAs under first-order phase transitions. In addition, taking all these singularities into account, we postulate for the first-order phase transition in CrAs a mechanism connected with the restructuring of its electron structure.

We recall that CrAs has a $B31$ crystal lattice that is a distorted $B8_1$ hexagonal close packed structure. The cation sublattice of its unit cell, with the indicated distances between the chromium atoms, according to the data of Boller and Kallel,[3] is shown in Fig. 3. It was on the basis of these x-ray data that we constructed the band scheme of CrAs (Figs. 4a and 4b).

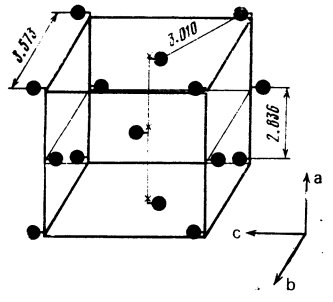

FIG. 3. Cation sublattice of unit cell of chromium arsenide in accordance with Ref. 3.

The outer $4s$ electrons of chromium, as well as the $4s$ and $4p$ electrons of arsenic, form on account of the strong covalent band a broad filled valence band (binding states) and an unfilled conduction band (antibinding states). The energy gap between these bands is large enough to prevent even a semiconducting conduction mechanism (according to the data of Ref. 11, for MnAs, which is close in its electronegativity, the width of this forbidden band is 3 eV). Thus, the outer s and p electrons cannot participate in the electric conductivity of CrAs.

We assume that the chromium ion in the investigated compound is trivalent, since $2d$ electrons "go off" to form a band with the p electrons of the arsenic. This leaves three $3d$ electrons per atom of chromium and at this configuration the crystal field of cubic symmetry O_h splits the fivefold degenerate (disregarding spin degeneracy) level of the free atom of chromium into two: a deadly degenerate level of symmetry e_g, and triply degenerate level of symmetry t_{2g}. The single-electron wave functions of symmetry e_g(d_{z2} and $d_{x^2-y^2}$) are directed towards the anion atoms and form a sufficiently broad band because of the strong covalent bond and because of hybridization with the s and p states (band $a_4 + a_5$ on Fig. 4a). On going from the cubic to the trigonal ligand-field symmetry D_{3h}, which is a property of the $B8_1$ structure, these bands remain practically unchanged. In the B31 lattice, however, the orthorhombic distortions take place in such a way (Fig. 3) that one can speak of two crystal sublattices compared with the more symmetrical structure of the $B8_1$ type. Such a distortion of the ligand octahedron splits the e_g bands into two bands shifted relative to each other. Since these bands are not filled and play no important role in the properties of CrAs, they are represented in our bands scheme by a single broad band $a_4 + a_5$.

A much greater influence is exerted by the orthorhombic distortions on the t_{2g} levels. The wave functions of these states have symmetries d_{xy}, d_{yz}, and d_{xz}. The d_{xy} lobes are directed towards the neighboring chromium atoms along the a axis, the distance between which in the LT phase is 2.836 Å. Since the Mott critical distance[12] R_c for the LS and CS of the $3d$ electrons in chromium amounts to[3] 3.18 Å, a strong covalent bond should exist between the indicated cations, and they should form a broad band of collectivized electrons (a_1 on Fig. 4a).

The interatomic distances between the nearest cations along the c axis and the LT phase (3.014 A) are close to $R_c = 3.18$ Å, and therefore the weak overlap of the wave functions of the atoms in this direction produces a very narrow band (a_2). The lowering of the symmetry of the ligand field in the B31 lattice compared with $B8_1$ manifests itself in the fact that the bands a_1 and a_2 are split into subbands of binding and antibinding states (the latter are designated a_1^* and a_2^*). The high state density in the narrow bands a_2 and a_2^* and the high correlation energy of the electrons in them can lead to a spontaneous band magnetism[9] and then it is precisely these bands which are responsible for the experimentally obtained localized magnetic moment $1.7\mu_B$ per chro-

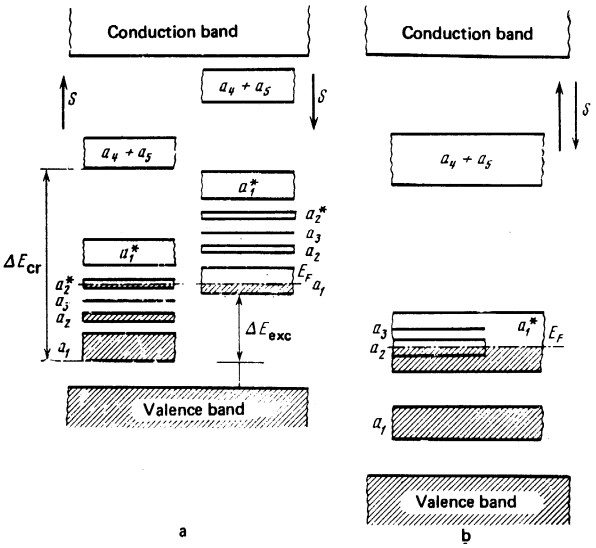

FIG. 4. Band scheme of chromium arsenide: a) low-temperature helicoidal magnetic phase (LS); b) high-temperature paramagnetic phase (CS). ΔE_{cr}—splitting due to the crystal field; ΔE_{exc}—exchange splitting. The arrows mark the directions of the spins in the left and right parts of the scheme.

mium atom. If this is so, the presence of this magnetic moment leads to additional lifting of the level degeneracy in the spin direction. On the band scheme this is manifest in the fact that the right-hand and left-hand parts of Fig. 4a are shifted by an amount equal to the intraatomic exchange energy ΔE_{exc}.

The local level E_F is connected with cations arranged along the b axis and spaced so far apart (3.573 Å) that their wave functions of the $3d$ electrons do not overlap. The Fermi level E_F should lie between the valence band and the conduction band, and we have placed it in such a way that it passes over the bands $a_{2\uparrow}^*$ and $a_{1\downarrow}$. This placement of E_F makes it possible to distribute the electrons and the bands in the following manner: $n_{a_{1\uparrow}} = 0.5$; $n_{a_{2\uparrow}} = 0.5$; $n_{a_{3\uparrow}} = 1$; $n_{a_{2\uparrow}}^* = 0.35$, and $n_{a_{1\downarrow}} = 0.65$. If we recognize that in the a_1 band the electron spin direction is opposite to that in the other bands, then the combined magnetic moment of the three $3d$ electrons of the chromium atom is $1.7\mu_B$ as is in fact observed in experiment. In addition, the narrow band $a_{2\uparrow}^*$, which is responsible for the presence of the magnetic moment, is less than half-filled. This should lead to an antiferromagnetic coupling between the cations that are arranged along the c axis.[13] This was precisely the coupling observed in the investigation of the magnetic structure of the DH of CrAs.[2] Partial filling of the bands $a_{2\uparrow}^*$ and $a_{1\downarrow}$ explains also the experimentally observed metallic character of the electric conductivity of CrAs, the mechanism of which will be considered in greater detail below (see sec. 4B).

We call attention to the fact that in the LT phase the local level $a_{3\uparrow}$ is filled, and the distances between the cations along the b axis are so large that the only interaction between their electron shells can be electrostatic repulsion. With increasing temperature, this distance decreases[3] because of the additional distortions of the unit cell due to heating. The energy of the electrostatic repulsion then increases, and the energy of the level $a_{3\uparrow}$ increases correspondingly, bringing this level closer to the bottom of the $a_{2\uparrow}^*$ band. At the temperature T_N the gap between the bands $a_{2\uparrow}^*$ and $a_{3\uparrow}$ decreases to such an extent that thermal transfer of the electron from band $a_{3\uparrow}$ to band $a_{2\uparrow}^*$ is possible. As soon as the level $a_{3\uparrow}$ becomes free, the causes of the repulsion of the atoms along the b axis disappear and the distance between them shortens abruptly to 3.445 Å. This leads to a lattice distortion such that the distances between the atoms along the c axis decrease to 3.010 Å $\ll R_c$, the $a_{2\uparrow}^*$ band broadens, the electrons in this band become collectivized, ΔE_{exc} drops abruptly, and the compound goes over into the state of Pauli paramagnetized via a first-order phase transition. The band picture corresponding to this state is shown in Fig. 4b. This, in our opinion, is the mechanism of the first-order phase transition in CrAs.

It should be noted that although this band scheme is quite approximate, it is based on conclusions of the crystal-field theory and explains adequately practically all the experimental data at our disposal. In particular,[14] the compressibility in the LT phase of CrAs is practically isotropic and positive, and at $T > T_N$ it is patently anisotropic also along the b axis and has the largest value, $K_b = +(2.8 \pm 0.08) \times 10^{-12}$ cm^2/dyn. In light of our band model, this phenomenon may be due to the fact that in the HT phase the fact that the a_3 level is not filled and that there is no electrostatic repulsion between the corresponding atoms allows the unit cell to be easily compressed in this direction.

Taking the foregoing into account, we shall use hereafter this band scheme to explain our experimental results.

When hydrostatic pressure is applied, the overlap of the $3d$ wave functions increases, broadening thereby all the d bands. The broadening of the $a_{2\uparrow}^*$ band, and correspondingly the decrease of the state density on the Fermi level in this band, leads to collectivization of the electrons and to a decrease of ΔE_{exc}. As a result, the magnetic-ordering temperature should shift under pressure towards lower temperatures, in agreement with our experimental data.

B. Conduction mechanism and calculation of the width of the CrAs band

As noted in Sec. 3, the dependence of the electric resistance of CrAs on the temperature is metallic both before and after the transition at all pressures. Our band scheme explains this behavior of the $R(T)/R_0$ plots.

In the LT phase (Fig. 4a), the Fermi level E_F lies in the overlapping bands $a_{2\uparrow}^*$ and $a_{1\downarrow}$. Since the width of the $a_{2\uparrow}^*$ band is much less than that of $a_{1\downarrow}$, it can be assumed in analogy with the Mott s–d conductivity[15] that the d electrons of the $a_{1\downarrow}$ band occupy under the influence of the electric field not only states above E_F in their own band, but also numerous free states of the band $a_{2\uparrow}^*$ with high state density.

In the HT phase (Fig. 4b), the bands a_1^*, a_2, and a_3 overlap, and the Fermi level E_F is located inside this

broad band, ensuring again metallic conduction. Just as in the LT phase, the state density in the band a_2 is much higher than in the band a_1^*, therefore the mechanism of the conduction at high temperatures similar to that in the LT phase. In other words, since $m_\alpha^* \gg m_\beta^*$ (where m_α^* and m_β^* are the effective masses of the d electrons of the a_2 and a_1^* bands), the "light" d electrons of band a_1^* are scattered by the "heavy" holes of band a_2.

The Mott $s-d$ scattering plays an important role only for paramagnetic-metal conduction electrons, while in the region where the material has magnetic order there is additional scattering by the magnetic spin structure. Therefore in the arguments and calculations that follow we shall use the notation of Fig. 4b, which shows the band scheme of chromium arsenide in the paramagnetic state.

If we accept the discribed mechanism of conduction in CrAs, we can use the two-band formula

$$\sigma = ne^2\left(\frac{\alpha\tau_\alpha}{m_\alpha^*}+\frac{\beta\tau_\beta}{m_\beta^*}\right), \tag{1}$$

where τ_α and τ_β are the relaxation times, and α and β are the relative numbers of the conduction electrons in bands a_2 and a_1^*, respectively. In both bands there is a total of n electrons per cm^3. Since $m_\alpha^* \gg m_\beta^*$, the first term in the parentheses can be neglected. In addition, recognizing that the conduction is produced by the electrons located in a narrow energy interval near E_F, while the state density of band a_2 is much higher than that of a_1^*, we see that $1/\tau_\beta$ is proportional only to the state density on the Fermi level $dN(E_F)/dE$ in the band a_2. In analogy with the Mott $s-d$ scattering we obtain for the temperature dependence of the relaxation time τ_β (Ref. 15)

$$\tau_\beta = A_\beta\left(1+\frac{\pi^2T^2}{6T_0^2}+\ldots\right)\Big/ T. \tag{2}$$

Here A_β is a coefficient inversely proportional to $dN(E_F)/dE$ in the a_2 band, and $kT_0 = E_F - E_0$ is the energy difference between E_F and the bottom E_0 of this band. Neglecting the fact that in the derivation of this equation we used a parabolic state-density function, we can approximately assume that $2kT_0$ gives the value of the width of the band a_2.

Combining (2) and (1), we obtain

$$\sigma T = \alpha n e^2 A_\beta\left(1+\frac{\pi^2T^2}{6T_0^2}\right)\Big/ m_\beta^*. \tag{3}$$

Since we have measured the relative resistance, we obtain, dividing both sides of (3) by $\sigma_0 = \sigma(224\ \text{K})$

$$\frac{\sigma T}{\sigma_0} = C_\beta\left(1+\frac{\pi^2T^2}{6T_0^2}\right), \quad C_\beta = \frac{\alpha n e^2 A_\beta}{\sigma_0 m_\beta^*}.$$

From the experimental $R(T)/R_0$ curves we plot $\sigma T/\sigma_0$ against T^2, and the intercepts of the obtained straight lines with the $\sigma T/\sigma_0$ axis yields the value of C_β for each pressure. We then get from (3)

$$T_0 = \left[\frac{\pi^2T^2}{\sigma(\sigma T\sigma_0^{-1}C_\beta^{-1}-1)}\right]^{1/2}; \tag{4}$$

$$\Delta E_\alpha \approx 2kT_0 \approx 2k\left[\frac{\pi^2T^2}{\sigma(\sigma T\sigma_0^{-1}C_\beta^{-1}-1)}\right]^{1/2}. \tag{5}$$

Figure 5 shows the plots of $\sigma T/\sigma_0$ against T^2 for the LT region. As indicated above, Eq. (5) is valid only for the paramagnetic state of CrAs. In fact, we could calculate the width of the a_2 band only starting with a certain pressure at which the magnetic order vanishes. This pressure turned out to be $P = 4.3$ kbar, and at lower pressures the derivatives $d(\sigma T/\sigma_0)/dT^2$ were negative and could not be used in the calculations inasmuch as expression (5) lost its physical meaning. As seen from Fig. 5, the linear sections obtained from the experimental curves increase with increasing pressure, and at $P = 9$ kbar the function is linear in practically the entire temperature interval. Analogous functions were applied also for the HT phase at all pressures.

With the aid of (5) we calculated from the straight lines of Fig. 5 the band width ΔE_α. The results of this calculation are shown in Fig. 6, where curve 1 gives the change of the width of this band under pressure in the HT region, while curve 2 gives the change of the width ΔE_α at low temperatures. It is seen that these curves are quite different.

In the HT phase (curve 1 of Fig. 6), where CrAs is paramagnetic at low pressures, ΔE_{HT} remains practically unchanged up to 2 kbar, and with further increase of pressure it increases and reaches the value 0.16 eV at $P = 9$ kbar. This corresponds to the usual influence of pressure on a Pauli paramagnet, i.e., the a_2-band width due to the overlap of the wave functions of the $3d$ electrons along the c axis increases smoothly with decreasing distance between the atoms in this direction.

The situation is more complicated in the case of the LT phase (curve 2 of Fig. 6). As shown above (Fig. 1), the highest pressure at which an abrupt first-order transition can be seen is 3.5 kbar. Obviously, at lower pressures ΔE_{LT} is very small and changes little with pressure, as shown in Fig. 6 by the dashed line. When the pressure increases to 4.3 kbar, ΔE_{LT} is 0.015 eV. It is seen that this is the critical value of the width of the a_2^* band (Fig. 4a) at which the Friedel criterion is not satisfied, the $3d$ electrons become collectivized, and the first-order magnetic phase transition vanishes. It is precisely this pressure (or at this critical band

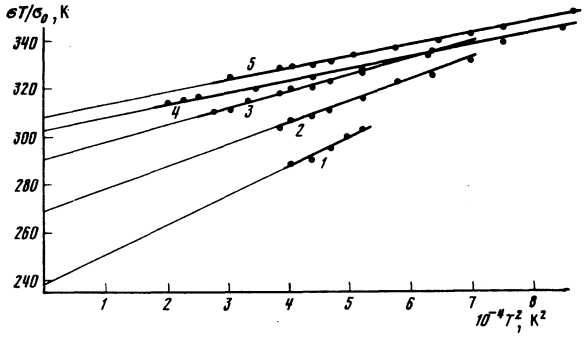

FIG. 5. Plots of $\sigma T/\sigma_0$ against T^2 obtained for the LT region from the experimental plots of $L(T)/R_0$ at various pressures P, kbar: 1—4.3; 2—5.5; 3—6.4; 4—7.5; 5—9.0.

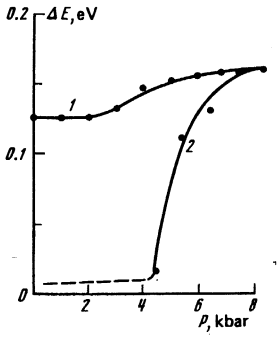

FIG. 6. Dependence of the width of band a_2 on the pressure in the high temperature (1) and in the low temperature (2) phases.

width) that we go from the helicoidal magnetic state of CrAs shown in Fig. 4a to the paramagnetic state (Fig. 4b), and the a_2^*, band is correspondingly transformed into the a_2 band.

Notwithstanding the collectivization of the d electrons in the a_2 band, at this pressure the local level a_3 is filled and is located below the Fermi level. With increasing temperature, its energy increases because of the repulsion of the atoms along the b axis, and at $T \sim 170$ K it crosses E_F, causing a redistribution of the electrons in the bands a_2 and a_1^* and structural distortions, just as indicated above in the description of the spontaneous first-order transition at atmospheric pressure (Sec. 4a). This is precisely the reason why at $P = 4.3$ kbar the band width ΔE_{LT} changes with increasing temperature from 0.015 eV in the LT region to 0.14 eV at high temperatures, as seen in Fig. 6, while curves 6 and 7 of Fig. 1 show gently sloping anomalies. The abrupt increase of ΔF_{LT} is due to the increase of the overlap of the wave functions of the d electrons along the c axis when higher pressures are applied. At $P = 6$ kbar, ΔE_{LT} is close to ΔE_{HT}, in the anomalies on the $R(T)/R_0$ curves vanish completely. At this pressure the level a_3 occupies at low temperatures a position higher than the Fermi level E_F, as shown in Fig. 4b, and no alteration of the band structure takes place with increasing temperature. With further increase of the pressure, ΔE_{LT} tends asymptotically to the linear function $\Delta E_\alpha(P)$ and at $P = 7$ kbar we already have $\Delta E_{LT} = \Delta E_{HT} = 0.16$ eV.

Even though this interpretation of our experimental data is quite approximate, it does explain the nature of the first-order phase transition in CrAs and the anomalous behavior of $R(T)/R_0$ under hydrostatic pressure. Berner[16] *et al.*, in an investigation of the optical reflection spectra in MnAs found that the widths of the narrow d bands fluctuate between 0.5 and 0.1 eV. This range, taking into account the proximity of the MnAs and CrAs crystal structures, is quite compatible with our results.

[1]N. Kazama and H. Watanabe, J. Phys. Soc. Jpn. **30**, 1319 (1971).
[2]K. Selte, A. Kjekshus, W. E. Jamison, A. F. Andresen, and J. E. Engebretsen, Acta Chem. Scand. **25**, 1703 (1971).
[3]H. Boller and A. Kallel, Solid State Commun. **9**, 1699 (1971).
[4]E. A. Zavadskiĭ and I. A. Sibarova, Fiz. Tverd. Tela (Leningrad) **18**, 1736 (1976) [Sov. Phys. Solid State **18**, 1009 (1976)].
[5]C. P. Bean and D. S. Rodbell, Phys. Rev. **126**, 104 (1962).
[6]E. A. Zavadskiĭ and I. A. Sibarova, Izv. Akad. Nauk SSSR Ser. Fiz. **42**, 1735 (1978).
[7]N. Menyuk, J. A. Kafalas, K. Dwight, and J. B. Goodenough, Phys. Rev. **177**, 942 (1969).
[8]J. B. Goodenough, Magnetism and the Chemical Bond, Interscience, 1963.
[9]R. W. Rathenau and J. B. Goodenough, J. Appl. Phys. **39**, 403 (1968).
[10]J. B. Goodenough and J. A. Kafalas, Phys. Rev. **157**, 389 (1967).
[11]K. Bärner, R. Braunstein, and E. Chock, Phys. Status Solidi B **80**, 451 (1977).
[12]N. F. Mott, Proc. Phys. Soc. London Ser. A **62**, 416 (1949).
[13]J. B. Goodenough, Russ. transl. in: Teoriya ferromagnetizma metallov i splavov (Theory of Ferromagnetism of Metals and Alloys), IIL, 1965, p. 116.
[14]E. A. Zavadskiĭ and V. I. Kamenev, Fiz. Tverd. Tela (Leningrad) **20**, 933 (1978) [Sov. Phys. Solid State **20**, 541 (1978)].
[15]N. F. Mott and H. H. Wills, Proc. R. Soc. London Ser. A **156**, 368 (1936).
[16]K. Bärner, Phys. Status Solidi B **81**, 385 (1977).

Translated by J. G. Adashko